J Mol Model (2009) 15:1125–1132
DOI 10.1007/s00894-009-0466-5

ORIGINAL PAPER

Homology modeling of a novel epoxide hydrolase (EH) from Aspergillus niger SQ-6: structure-activity relationship in expoxides inhibiting EH activity

Quan Luo · Yuan Yao · Wei-Wei Han · Yi-Han Zhou · Ze-Sheng Li

Received: 4 November 2008 / Accepted: 10 January 2009 / Published online: 21 February 2009

Abstract The 3D structure of a novel epoxide hydrolase from Aspergillus niger SQ-6 (sqEH) was constructed by using homology modeling and molecular dynamics simulations. Based on the 3D model, Asp191, His369 and Glu343 were predicted as catalytic triad. The putative active pocket is a hydrophobic environment and is rich in some important non—polar residues (Pro318, Trp282, Pro319, Pro317 and Phe242). Using three sets of epoxide inhibitors for docking study, the interaction energies of sqEH with each inhibitor are consistent with their inhibitory effects in previous experiments. Moreover, a critical water molecule which closes to the His369 was identified to be an ideal position for the hydrolysis step of the reaction. Two tyrosine residues (Tyr249 and Tyr312) are able to form hydrogen bonds with the epoxide oxygen atom to maintain the initial binding and positioning of the substrate in the active pocket. These docked complex models can well interpret the substrate specificity of sqEH, which could be relevant for the structural—based design of specific epoxide inhibitors.

Keywords Epoxide hydrolase · sqEH · Homology modeling · Molecular docking · Enantio—selectivity

Introduction

Epoxides are well—known intermediates in the metabolism of many drugs, xenobiotics, and endogenous compounds. Because of their electronic polarization and ring tension, epoxide metabolites are highly reactive compounds and can cause cancer by forming covalent adducts with DNA [1–3]. Epoxide hydrolases (EHs), which belong to the α/β hydrolase family [4–5], can catalyze the hydrolysis of epoxides to the less toxic vicinal diols via a two—step mechanism involving the formation and hydrolysis of a covalent intermediate [6–7]. These enzymes are found in various organisms, such as bacteria, fungi, plants and insects [8–10]. The different epoxide hydrolases exhibit different substrate specificities, region—and enantioselectivities, which make them potentially useful as biocatalysis for the chiral synthesis of fine chemicals [11].

In mammals, at least five classes of epoxide hydrolases have been recognized, especially for soluble epoxide hydrolase (sEH) and microsomal epoxide hydrolase (mEH) [12, 13]. Nevertheless, a commercial interesting fungal EH from Aspergillus niger SQ-6, exhibiting significant sequence homology with mammalian mEH, has drawn much attention for its highly enantioselectivity with chiral epoxides [14–16]. Very recently, the gene of the novel epoxide hydrolase (sqEH) was cloned and expressed [17]. Sequences alignment has shown that sqEH shares 59% amino acid sequence identity with epoxide hydrolase from the fungus Aspergillus niger (AnEH), whose three—dimensional structure is the first solved structure of the mEH family. According to the experimental report, three classes of epoxide inhibitors including aromatic epoxides, aliphatic epoxides and cyclic expoxides were investigated by measuring their inhibitory effects on the rate of hydrolysis of p—nitrostyrene oxide (pNSO), whereas sqEH can hydrolyze only aromatic and aliphatic epoxides efficiently and showed strict specificity toward (R)—enantiomer [17].

Q. Luo · Y. Yao · W.-W. Han · Y.-H. Zhou · Z.-S. Li (✉)
State Key Laboratory of Theoretical and Computational Chemistry, Institute of Theoretical Chemistry, Jilin University, Changchun 130023, People's Republic of China
e-mail: zeshengli@mail.jlu.edu.cn

Due to the lack of the three—dimensional (3D) structure of sqEH, the detailed mechanism of interaction of sqEH with epoxide inhibitors remains unclear. In this paper, the 3D model of sqEH was constructed by using microsomal epoxide hydrolase AnEH as a template [18]. Substrate pNSO and eight epoxide inhibitors have been simulated to interact with sqEH model, respectively, to study their binding mechanism, which will help to improve the potency and selectivity of the inhibitors.

Theory and methods

Homology model construction

BLAST program search [19] showed that sqEH and AnEH (PDB ID: 1QO7) share many common sequence features. Multiple sequence alignment [20] was subsequently performed to predict their structure—conserved regions (SCRs). Copying the backbone coordinates of the SCRs from template AnEH, and exploring the conformations of side chains by using Auto_Rotamers [21–22], the initial structure of sqEH was built by using the Insight II package [23].

The further optimization protocol involves multiple—step energy minimization and molecular dynamics (MD) simulation for fully relaxing our initial model. All simulations were carried out through the Amber 9 program [24, 25] using the ff03 force field and periodic boundary conditions [26]. Chloride ions were added to neutralize the positive charge of the system, and the protein was solvated with a 8 Å TIP3P water cap. Prior to MD simulations, two steps of minimization were performed. First, the protein sqEH was fixed with a restraint of 500 kcal/mol·Å^2 and only the positions of waters and ions were minimized. Then, the entire simulation system was minimized. After the energy minimization, a 100 ps MD simulation was carried out at constant volume condition, and the temperature was heated up continuously from 0 to 300 K. The time step of the simulations was 2.0 fs with a cutoff of 12 Å for the nonbonded interaction, and SHAKE algorithm was used to constrain bonds involving hydrogen atoms. Finally, 3.9 ns of constant—pressure MD simulation was performed to equilibrate the entire system using Langevin thermostat at 300 K [27–29]. The final conformations of sqEH were obtained when the total energy reached the minimum. The best structure was examined by using Profile-3D [30, 31] and Procheck programs [32].

Binding—site analysis

The Binding—Site module [33] is a suite of programs in InsightII for identifying and characterizing protein active sites, binding sites, and functional residues from protein. In this study, ActiveSite—Search was used to search for the protein active site and binding site by locating cavities in the sqEH structure, which can be used to guide the protein—ligand docking experiment.

Flexible docking

The refined sqEH model was used to study its ligand binding mechanism. Substrate (pNSO) and three sets of epoxide inhibitors including aromatic epoxides (phenyloxirane, 4-methylphenyloxirane and 4-chlorophenyloxirane), aliphatic epoxide (1-hexyloxirane, 1-butyloxirane and 1-octyloxirane) and cyclic expoxides (cyclohexene oxide and cyclopentene oxide) were docked into the active—site pocket. Affinity, which uses a combination of Monte Carlo and simulated annealing method, was used to fulfill the automated molecular docking procedure [34]. The potential function of the complexes was assigned by using the consistent—valence force field (CVFF) and non—bonding interaction was dealt with the cell multipole approach. To consider the solvent effect, the centered enzyme—ligand complexes were solvated in a sphere of TIP3P water molecules with radius 5 Å, and the number of water molecules required slight adjustment to make them identical for all the ligands. Finally, the docked complexes of sqEH with each inhibitor were selected by the criteria of interaction energy combined with the geometrical matching quality. These complexes were used as the starting conformation for further energetic minimization and geometrical optimization before the final models were achieved [35, 36].

Results and discussion

Structure prediction of sqEH

The structure of sqEH is obtained by using homology modeling and molecular dynamics simulations and the final structure which is in accordance with the 'canonical' α/β hydrolase fold [37] is presented in Fig. 1. It is shown that the enzyme can be divided into two domains. The core domain is composed of a mostly parallel, eight—stranded β—sheet (named β1–β8, only the β2 is antiparallel) that is flanked on both sides by seven helices (αA–αG). The cap (or lid) domain contains six α helices corresponding to residues 230-316 (αD1–αD6). The superimposition of backbones of sqEH with AnEH protein gives the RMSD value of 0.57 Å, which means that they have a high similarity.

The overall quality of the final structure of sqEH model was examined by Profile-3D to see whether the structure is compatible with target sequence. Results showed that the

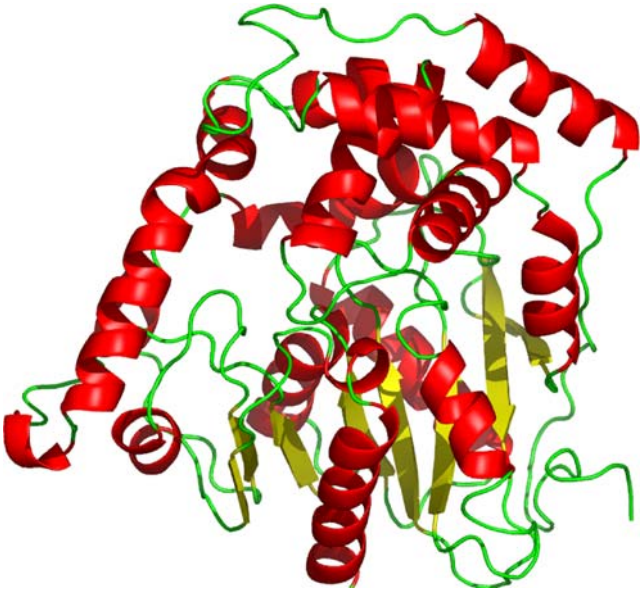

Fig. 1 The three-dimensional structure of the refined sqEH model

sum of the self—compatibility score for this model is 180.8 which is a little higher than the expected score for a correct structure (180.1). Furthermore, Shown as the graph of the local compatibility score S (Fig. 2 a), the conformation of each residue is considered to be validity as their compatibility scores are positive. Procheck was used to calculate the backbone φ, φ torsion angles of sqEH model. The percentage of residues within allowed regions in Ramachandran plot is 100% (Fig. 2 b) which indicate that the stereochemical quality of our model is quite reasonable.

Determination of the putative binding pockets of sqEH

To define the catalytic residue for sqEH, multiple sequence alignment was performed to analyze the conserved amino acid residues between sqEH and AnEH. Based on the alignment results, sqEH shows 59% amino acid sequence identity with AnEH and contains some highly conserved amino acid residues forming the catalytic triad nucleophile acid, represented by aspartic acid at position 191, glutamine at position 343, and histidine at position 369. The catalytic nucleophile Asp191, which is located in the sharp turn (Gly—Gly—Asp191-Ile-Gly, a "nucleophile elbow" in α/β hydrolase fold enzymes) between strand β5 and helix αF of the core domain, was observed to be strained (Fig. 2 b). This is an energetically unfavorable conformation observed in hydrolases and is believed to provide an energy reservoir for catalysis.

The binding—site was searched by Binding—Site module. The largest pocket containing Asp191 was determined to be the binding site. As shown in Fig. 3, the backbone of sqEH is well superimposed on that of template AnEH, whereas the superposition reveals that the binding pocket of sqEH is apparently different from that observed in AnEH. The putative pocket for sqEH has a deep channel, which provides a hydrophobic environment for substrate and is rich in non—polar residues Trp216, Phe242, Ala243, Trp282, Pro317, Pro318, Pro319, Leu344 and Val345.

Docking of the inhibitor into the active site

All molecules (R—enantiomer), including substrate and the series of epoxide inhibitors as listed in Table 1, were docked into sqEH model by means of the Affinity program.

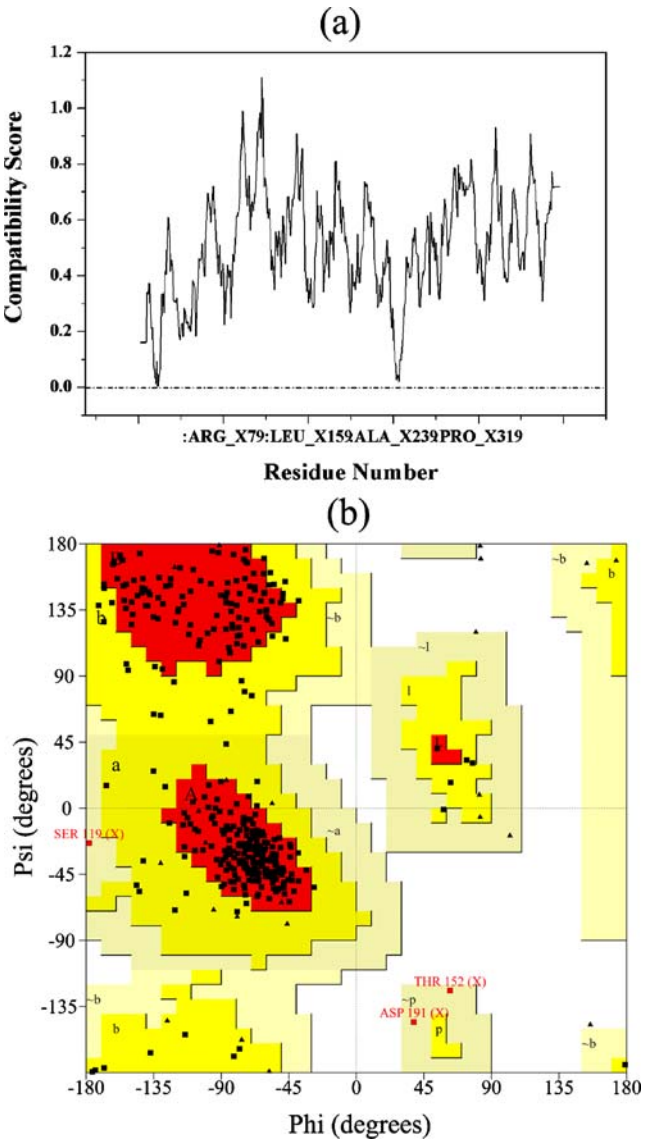

Fig. 2 (**a**) 3D profiles of verified results of the refined sqEH model. (**b**) Ramachandran plot of the refined sqEH model. The most favored regions are colored in red. Allowed, generously allowed, and disallowed regions are indicated as yellow, light yellow and white regions, respectively. The residues in the disallowed region are marked in red

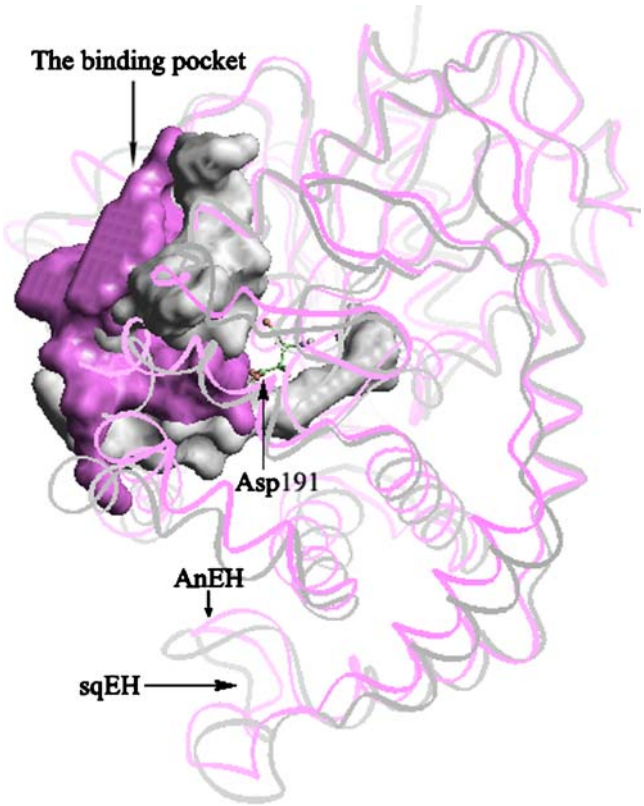

Fig. 3 Comparison of refined sqEH model with its template protein AnEH. (Magenta ribbon, AnEH; Grey ribbon, SABP2) The binding pocket of them exhibit different shape

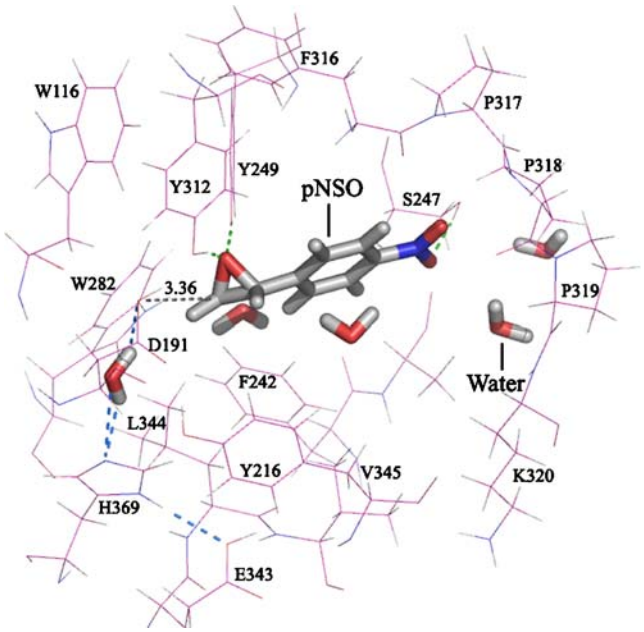

Fig. 4 (R)-pNSO docked into the refined sqEH model. The most important hydrogen-bonding interactions displayed. One water molecule near the His396-Glu343 pair is thought to be involved in the hydrolysis reaction

Figure 4 shows the detailed binding mode between substrate (pNSO) and sqEH model. Both Tyr249 and Tyr312 can form hydrogen bonds with the oxygen of pNSO, their participation in ligand binding are important for anchoring the epoxide moiety of substrate, and the presence of two tyrosine residues previously identified as conserved residues in all known mammalian EH sequences. Furthermore, the oxygen and nitrogen of the nitro group in pNSO are hydrogen bonded to the hydroxyl of Ser247. This interaction is beneficial for the docking orientation of the phenyl ring of pNSO which is located in a hydrophobic environment. The side chain hydroxyl of the catalytic nucleophile Asp191 is located with a distance of 3.36 Å to the carbon of epoxide moiety of pNSO in a perfect position for initiating the nucleophilic attack. However, the distance between O atom in Asp191 and the backbone N atom of His369 is 5.74 Å, and Asp191 can not form the hydrogen—bonding network to constitute a catalytic triad. One water molecule near the charge—relay residues (His369 and Glu343) is speculated to be important in ligand binding. Acting as either a hydrogen—bond donor or acceptor, the

Table 1 Docking several epoxide inhibitors into the binding pocket of sqEH model using affinity program. The total interaction energy between enzyme and each inhibitor was reported

Compound	E_{vdw} (kcal mol^{-1})	E_{ele} (kcal mol^{-1})	E_{total} (kcal mol^{-1})	Inhibition rate (%)
pNSO	−28.34	−11.47	−39.81	100
Phenyloxirane	−18.93	−11.83	−30.76	68±3
4-Methylphenyloxirane	−14.42	−12.27	−26.69	58±3
4-Chlorophenyloxirane	−23.70	−12.07	−35.77	85±3
1-Hexyloxirane	−20.77	−11.83	−32.59	23±4
1-octyloxirane	−25.93	−11.93	−37.86	78±2
1-butyloxirane	−16.39	−12.11	−28.50	0
Cyclohexene oxide	36.41	−12.25	24.16	0
Cyclopentene oxide	24.17	−11.25	12.92	0

water molecule can form a hydrogen bond with the carboxylic acid group of Asp191 and the imadazole ring of His369, respectively. This suggested that the water molecule is ideally positioned for the hydrolysis step of the reaction, and we propose a catalytic mechanism for sqEH (Fig. 5) in which the reaction is believed to occur in two steps: I) The carboxylate side chain of the catalytic nucleophile Asp191 attacks the Cα of the epoxide ring, leading to the formation of a covalent ester intermediate. This process is facilitated by one of tyrosine residues (Tyr249 and Tyr312) which can act as proton donors for the epoxide ring oxygen and assist in ring opening; II) One water molecule activated by the His396—Glu343 pair via proton abstraction finally hydrolyses the ester intermediate to product.

To determine the other key residues in binding pocket of the model, the interaction energies of pNSO with sqEH are calculated. Table 1 gives the interaction energies including the total energies, van—der—Waals, and the electrostatic energies; the residues which are within a sphere defined by 5 Å radius around the central molecular (pNSO) were recorded as well (Table 2). The complex has favorable total interaction energy of -39 kcal mol^{-1}, the van-der-Waals (vdW) and electrostatic energies are -28.34 and -11.47 kcal mol^{-1}, respectively. It means that the interaction is mainly attractive interaction. From Table 2 we also know that Pro318, Trp282, Pro319, Pro317 and Phe242 have important contributions to the substrate binding and the side chains of these residues can provide a rather vdW interaction with substrate to stabilize the phenyl ring of pNSO.

According to experimental report, the enzyme sqEH showed strict specificity toward (R)—enantiomer. We have modeled the binding of (S)—pNSO into the active site to study the different direction of attack by Asp191 on the two enantiomers. As shown by Fig. 6, the S isomer is placed in a similar position to (R)—pNSO in which the epoxide oxygen atom is anchored by two hydrogen bonds donated by Tyr249 and Tyr312. However, the plane of the epoxide ring is aligned quite differently with respect to the catalytic nucleophile, and there would be a few steric clashes between the epoxide ring of (S)—pNSO and the residues in active—site pocket. This discovery was further confirmed by calculating the interaction energy. The results

Table 2 The total energy (E_{total}), van-der-Waals energy (E_{vdw}) and electrostatic energy (E_{ele}) between substrate pNSO and individual residues in sqEH

Residue	E_{vdw} (kcal mol^{-1})	E_{ele} (kcal mol^{-1})	E_{total} (kcal mol^{-1})
Try249	−2.82	−3.94	−6.76
Try312	−0.87	−5.86	−6.73
Ser247	−2.36	−2.67	−5.03
Asp191	−0.05	−3.12	−3.17
Pro318	−2.86	0.57	−2.29
Trp282	−1.76	−0.48	−2.24
Pro319	−2.04	0.16	−1.88
Pro317	−2.30	0.45	−1.85
Phe242	−2.04	0.27	−1.77
Val345	−0.29	−0.03	−0.32
Leu344	−0.60	0.31	−0.29
Try216	−0.79	0.53	−0.26
Ala243	−0.35	0.12	−0.23

* The residues within 5 Å radius around pNSO listed in energy rank order

with a positive total interaction energy 131.91 kcal mol^{-1} (vdW and electrostatic energies are 136.73 and -4.82 kcal mol^{-1}, respectively) imply that (S)—pNSO can not steadily bind with sqEH. Therefore, the enantio— and regio—selectivities of sqEH can presumably be explained in terms of the shape and character of the active—site cavity.

With regard to the docking of pNSO with the target protein, the binding analysis of other aromatic epoxides including phenyloxirane, 4-methylphenyloxirane and 4-chlorophenyloxirane with sqEH were performed. Similarly, these aromatic epoxides interact with the binding site of sqEH forming H-bond with Tyr249 and Tyr312. The phenyl ring is stabilized by hydrophobic interactions with Pro318, Trp282, Pro319, Pro317 and Phe242. As shown in Table 1, reporting the total interaction energy for each ligand versus the experimental inhibitory effects, there is quite a good correlation [17], the maximum total interaction energy value of -26.69 kcal mol^{-1} being associated with the low active compound 4-methylphenyloxirane and the minimum total interaction energy value of -35.77 kcal mol^{-1} being associated with the high active compound 4-

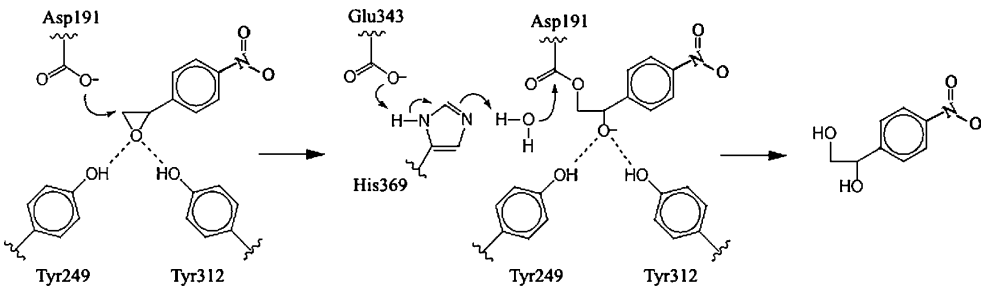

Fig. 5 The proposed catalytic mechanism for sqEH

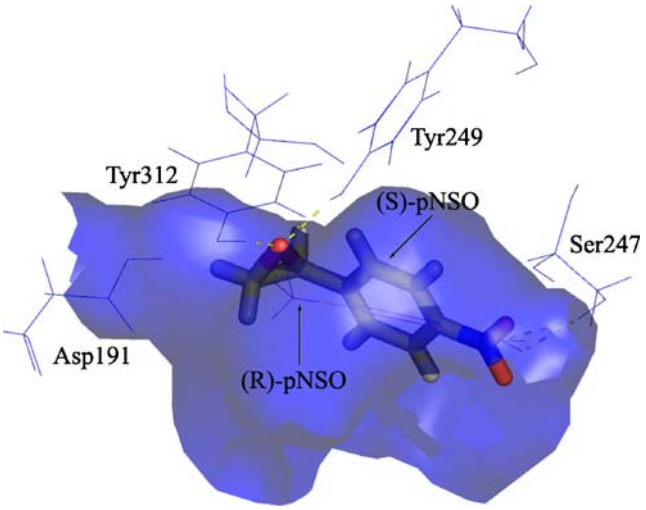

Fig. 6 The enantiomers of pNSO docked into the active site of the enzyme sqEH, shown with a solvent accessible surface. Stick, (S)-pNSO; Line, (R)-pNSO

Table 3 The total energy (E_{total}), van-der-Waals energy (E_{vdw}) and electrostatic energy (E_{ele}) between inhibitor 1-hexyloxirane and individual residues in sqEH

Residue	E_{vdw} (kcal mol^{-1})	E_{ele} (kcal mol^{-1})	E_{total} (kcal mol^{-1})
Try312	−0.91	−5.84	−6.75
Try249	−1.63	−3.68	−5.31
Asn315	−3.13	−0.48	−3.61
Lys320	−2.61	−0.05	−2.66
Tyr216	−2.54	0.17	−2.37
Asp191	−0.57	−1.05	−1.62
Pro318	−1.24	−0.23	−1.47
Pro319	−1.04	−0.09	−1.13
Trp282	−0.74	−0.32	−1.06
Lys195	−0.66	0.06	−0.60
Phe242	−0.27	0.08	−0.19
Val345	−0.20	0.01	−0.19
Leu344	−0.28	0.09	−0.19
Ser247	−0.29	0.13	−0.16

* The residues within 5 Å radius around1-hexyloxirane listed in energy rank order

chlorophenyloxirane. The difference in interaction energy between the three docked compounds is apparently caused by the functional group on the phenyl ring. Substituting a chlorine atom for nitro group, 4-chlorophenyloxirane can not form a hydrogen bond with the hydroxyl of Ser247, leading to an increase of 4.64 kcal mol^{-1} in vdW interaction energy relative to pNSO, whereas the chlorine—substituted benzene ring compound has a higher affinity and stronger binding capacity than phenyloxirane, which is attributed to the polar interaction between the chlorine atom of ligand and receptor. 4-methylphenyloxirane, with a relatively large methyl group, tends to produce some steric hindrance with Ser247, and makes an increase of 4.51 kcal mol^{-1} in vdW interaction energy relative to phenyloxirane. Thus, we think that these aromatic epoxides are competitive inhibitor for sqEH, in which the polar and the size of the substituted group on the phenyl ring can well elucidate the change of the inhibitory effects.

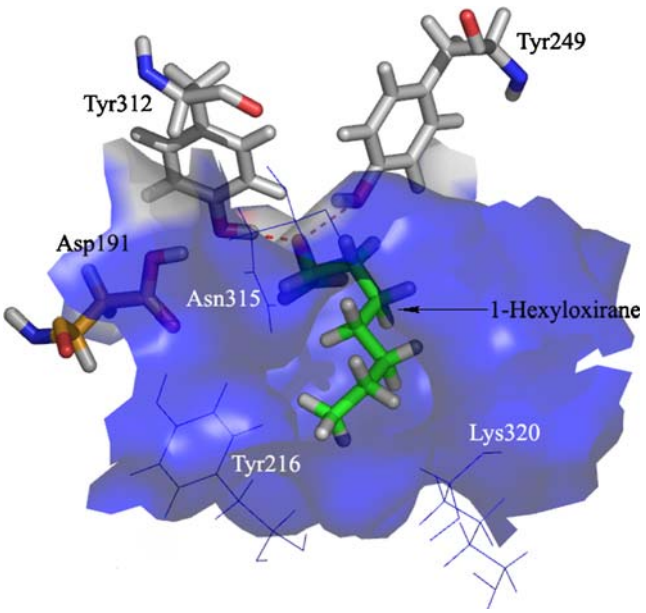

Fig. 7 Docking of 1-hexyloxirane to the binding pocket of sqEH. The long aliphatic chain is mainly interacting with Asn315, Lys320 and Tyr216

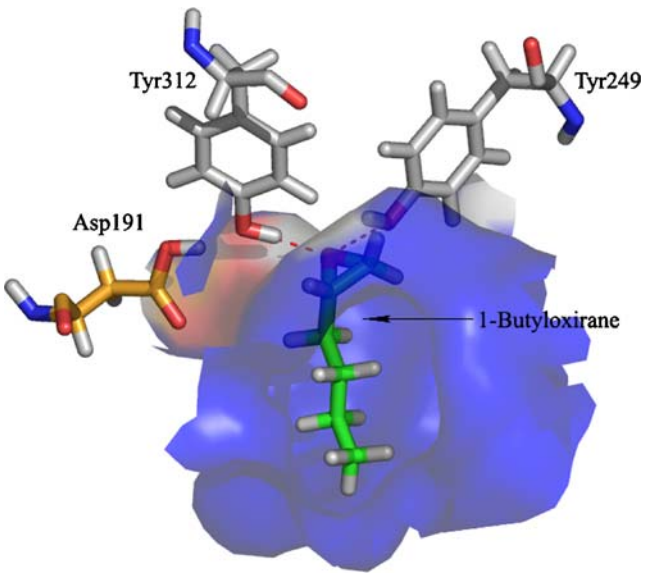

Fig. 8 Docking of 1-butyloxirane to the binding pocket of sqEH. The plane of the epoxide ring has turned nearly 90 degrees relative to that of 1-hexyloxirane in sqEH model

With the success of docking aromatic epoxides to our sqEH model, we extended the ligand binding study to aliphatic epoxide. Through interaction energy analysis, 1-hexyloxirane, one of these compounds, have a total interaction energy of -32.59 kcal mol^{-1}, in which the vdW and electrostatic energies are -20.77 and -11.83 kcal mol^{-1}, respectively. In general, the smaller total interaction energy, the greater the affinity an enzyme has for its substrate. Compared with the aromatic epoxides, the catalytic activity of 1-hexyloxirane should be much higher than those of 4-Methylphenyloxirane and Phenyloxirane. However, our docking result is not in harmony with the experimental inhibitory effect (Table 1). This problem can be explained by the structure of the hexyloxirane—sqEH complex model (Fig. 7). The absence of a phenyl ring, the orientation of the epoxide ring in 1-hexyloxirane has changed a little as the long aliphatic chain goes through a long channel and interacts with the residues in the channel of the active—site pocket. The distance from the hydroxyl oxygen atom of catalytic nucleophile Asp191 to the Cα atom of epoxide ring has elongated 0.61 Å relative to that in (R)—pNSO—sqEH complex which is 3.36 Å. This distance change is not favorable to the Asp191 nucleophilic attack and results in an apparent decreased inhibitory effect to1-hexyloxirane. Table 3 lists the detailed interaction energies of 1-hexyloxirane with the surrounding residues in sqEH. Obviously, the interactions with Try312 and Try249 are still maintained, and the long aliphatic chain is mainly interacting with Asn315, Lys320 and Tyr216 which is located on the entrance of the active—site pocket (Fig. 7).

Because the length of the aliphatic chain may affect the binding capacity of the ligands, the binding analysis of other aliphatic epoxides will provide us more information. Docking of 1-Octyloxirane into the active site, it binds to sqEH in a similar fashion to 1-hexyloxirane. However, the total interaction energy decreases to -37.86 kcal mol^{-1}, where the vdW and electrostatic energies are -25.93 and -11.93 kcal mol^{-1}, respectively. It is obvious that the electrostatic energy of 1-Octyloxirane and 1-hexyloxirane are nearly identical as Try312 and Try249 make a major contribution to the electrostatic energy supply, whereas the calculated vdW energy in 1-Octyloxirane is smaller than that in 1-hexyloxirane, which is due to the decreased interaction energy between ligand and the key residues on the entrance of active-site pocket, especially for the residue Asn315, whose value is -4.38 kcal mol^{-1}. This result is consistent with experimental data that the inhibitory effect of 1-Octyloxirane is stronger than that of 1-hexyloxirane (Table 1). 1-butyloxirane, on the other hand, also has favorable total interaction energy of -28.50 kcal mol^{-1} (vdW and electrostatic energies are -16.39 and -12.11 kcal mol^{-1}, respectively), but the inhibitory effect is zero, indicating that the docking orientation of the 1-butyloxirane may change dramatically. Figure 8 presents the binding model of 1-butyloxirane-sqEH complex. Both Tyr249 and Tyr312 still form a hydrogen bond with 1-butyloxirane, but the butyl chain moves away from the channel, leading the plane of the epoxide ring to turn nearly 90 degrees with respect to that of 1-hexyloxirane in sqEH model. Accordingly, the distance from the hydroxyl oxygen atom of catalytic nucleophile Asp191 to the Cα atom of epoxide ring has elongated to 5.34 Å, which is too long to initialize a nucleophile attack. Thus, replacement of the long aliphatic chain with a short aliphatic chain, the aliphatic epoxide will be correlated with a lower activity. This is in agreement with the experimental result that short chain aliphatic epoxides showed little effect on EH activity [17].

Finally, cyclohexene oxide and cyclopentene oxide were docked into the binding pocket. The volume of the binding pocket in sqEH reveals that there is no enough space around Try312 and Try249 to accommodate a bulkier ring, which will induce unfavorable vdW interaction energy for cyclohexene oxide (36.41 kcal mol^{-1}) and cyclopentene oxide (24.17 kcal mol^{-1}). The docking results with a positive total interaction energy suggest that these ligands can not steadily bind into the active site and exhibit any activity. This is consistent with the reported experimental result where the inhibitory effect of cyclohexene oxide and cyclopentene oxide on the rate of hydrolysis of pNSO is zero [17].

As discussed above, it is concluded that sqEH can hydrolyze only aromatic and long aliphatic epoxides efficiently and showed strict specificity toward (R)-enantiomer. The polar and the size of the substituted group on the phenyl ring play an important role in adjusting the inhibitory effect of aromatic epoxides.

Conclusions

In this study, the 3D structural model of sqEH has been constructed and optimized by MD simulation. The refined model has a reasonable residual distribution based on the analysis by Procheck and Profile-3D. Furthermore, three sets of epoxide inhibitors were docked into the sqEH model to study their binding modes and the possible catalytic mechanism. All the expected major interactions between the amino acids in active domain and the inhibitors were described in detail. These complex structures can well interpret the specificity of protein sqEH towards the substrates and provide valuable information to improve the potency and selectivity of the new inhibitors.

Acknowledgements This work was supported by the National Science Foundation of China (20333050, 20673044), PCSIRT (IRT0625), Key subject of Science and Technology by Jilin Province

and 985 Graduate Innovation Program of Jilin University (20080220). We also thank professor David A. Case et al for providing us the Amber 9 software as a freeware.

References

1. Arand M, Oesch F (2002) Wiley, New York, pp 459-483
2. Armstrong RN (1999) Drug Metab Rev 31:71–86
3. Oesch F (1973) Xenobiotica 3:305–340
4. Arand M, Wagner H, Oesch F (1996) J Biol Chem 271:4223–4229
5. Lacourciere GM, Armstrong RN (1993) J Am Chem Soc 115:10466–10467
6. Weijers CAGM, de Bont JAM (1999) J Mol Catal B Enzym 6:199–214
7. Armstrong RN, Cassidy CS (2000) Drug Metab Rev 32:327–338
8. Rink R, Fennema F, Smids M, Dehmel U, Janssen DB (1997) J Biol Chem 272:14650–14657
9. Arand M, Hemmer H, DSrk H, Baratti J, Archelas A, Furstoss R, Oesch F (1999) Biochem J 344:273–280
10. Wojtasek H, Prestwich GD (1996) Biochem Biophys Res Commun 220:323–329
11. Ready JM, Jacobsen EN (2001) J Am Chem Soc 123:2687–2688
12. Bell PA, Kasper CB (1993) J Biol Chem 268:14011–14017
13. Laughlin LT, Tzeng HF, Lin S, Armstrong RN (1998) Biochemistry 37:2897–2904
14. Moussou P, Archelas A, Furstoss R (1998) J Mol Catal B Enzym 5:447–458
15. Moussou P, Archelas A, Baratti J, Furstoss R (1998) Tetrahedron: Asymmetry 9:1539–1547
16. Cleij M, Archelas A, Furstoss R (1998) Tetrahedron: Asymmetry 9:1839–1842
17. Liu Y, Wu S, Wang J, Yang L, Sun W (2007) Protein Expr Purif 53:239–246
18. Zou J, Hallberg BM, Bergfors T, Oesch F, Arand M, Mowbray SL, Jones TA Structure 8:111–122
19. Altschul SF, Madden TL, Schäffer AA, Zhang J, Zhang Z, Miller W, Lipman DJ (1997) Nucleic Acids Res 25:3389–3402
20. Higgins DG, Bleasby AJ, Fuchs R (1992) Comput Appl Biosci 8:189–191
21. Ke YY, Chen YC, Lin TH (2006) J Comput Chem 27:1556–1570
22. Gui C, Zhu W, Chen G, Luo X, Liew OW, Puah CM, Chen K, Jiang H (2007) Proteins 67:41–52
23. Accelrys. InsightII, Version 2000, Homology User Guide. San Diego: Biosym/MSI
24. Case DA, Darden TA, Cheatham TE III, Simmerling CL, Wang J, Duke RE, Luo R, Merz KM, Pearlman DA, Crowley M, Walker RC, Zhang W, Wang B, Hayik S, Roitberg A, Seabra G, Wong KF, Paesani F, Wu X, Brozell S, Tsui V, Gohlke H, Yang L, Tan C, Mongan J, Hornak V, Cui G, Beroza P, Mathews DH, Schafmeister C, Ross WS, Kollman PA (2006) AMBER 9 University of California San Francisco
25. Case DA, Cheatham TE, Darden T, Gohlke H, Luo R, Merz KM, Onufriev A, Simmerling C, Wang B, Woods R (2005) The Amber biomolecular simulation programs. J Comput Chem 26:1668–1688
26. Ponder JW, Case DA (2003) Adv Prot Chem 66:27–85
27. Simmerling C, Strockbine B, Roitberg AE (2002) J Am Chem Soc 124:11258–11259
28. Pastor RW, Brooks BR, Szabo A (1988) Mol Phys 65:1409–1419
29. Tuccinardi T, Manetti F, Schenone S, Martinelli A, Botta M (2007) J Chem Inf Model 47:644–655
30. Accelrys. InsightII, Version 2000, Profiles-3D. San Diego: Biosym/MSI
31. Lüthy R, Bowie JU, Eisenberg D (1992) Nature 356:83–85
32. Laskowski RA, Macarthur MW, Moss DS, Thornton JM (1993) J Appl Crystallogr 26:283–291
33. Binding site analysis user guide. (2000) San Diego, USA: Accelrys, Inc
34. Affinity San Diego Molecular Simulations Inc (2000)
35. Bartlett PA, Shea GT, Telfer SJ, Waterman S (1989) R Soc Chem 182–196
36. Shoichet BK, Kuntz ID, Bodian DL (1992) J Comput Chem 13:380–397
37. Nardini M, Dijkstra BW (1999) Curr Opin Struct Biol 9:732–737